


Article

Research on High-Efficiency Transmission Characteristics of Multi-Channel Breast Ultrasound Signals Based on Graphene Structure

Xinsa Zhao , Jianning Han *, Peng Yang and Rongrong Zhao

School of Information and Communication Engineering, North University of China, Taiyuan 030051, China; s1905130@st.nuc.edu.cn (X.Z.); s1705069@st.nuc.edu.cn (P.Y.); s1805069@st.nuc.edu.cn (R.Z.)

* Correspondence: hanjn46@nuc.edu.cn

Abstract: In breast ultrasound CT imaging, the ultrasound signals received by high-density CMUT cylindrical array have problems of low transmission efficiency, susceptibility to interference from other signals, and an inability to achieve efficient acquisition. Therefore, to overcome these problems, based on acoustic metamaterials and graphene structure, an efficient transmission model of the multi-channel breast ultrasonic signals was designed, and a finite element simulation experiment was conducted. Research showed that the separation of ultrasonic signals could be achieved by the model designed in this article. The anti-interference ability in the ultrasonic signal acquisition process was effectively improved by the good multi-channel directional transmission and the sound wave local enhancement effect, which improved the sound wave transmission efficiency. In addition, the acoustic signals could be effectively transmitted from 80 kHz to 4000 kHz, realizing broadband transmission. Based on the flexibility of the design of the phononic crystal structure, phase adjustment could be achieved in a wide frequency range by changing the parameters of the primary cell structure. This enabled the CMUT cylindrical array to obtain better directivity characteristics, laying the foundation for high-quality breast ultrasound imaging.

Keywords: ultrasonic CT imaging; graphene structure; acoustic metamaterials; efficient transmission; CMUT



Citation: Zhao, X.; Han, J.; Yang, P.; Zhao, R. Research on High-Efficiency Transmission Characteristics of Multi-Channel Breast Ultrasound Signals Based on Graphene Structure. *Crystals* **2021**, *11*, 507. <https://doi.org/10.3390/cryst11050507>

Academic Editors: Zhimiao Yan, John Parthenios, Zhimiao Yan and Ting Tan

Received: 12 March 2021
Accepted: 30 April 2021
Published: 4 May 2021

Publisher's Note: MDPI stays neutral with regard to jurisdictional claims in published maps and institutional affiliations.



Copyright: © 2021 by the authors. Licensee MDPI, Basel, Switzerland. This article is an open access article distributed under the terms and conditions of the Creative Commons Attribution (CC BY) license (<https://creativecommons.org/licenses/by/4.0/>).

1. Introduction

In recent years, breast cancer has ranked first in the incidence of female tumors worldwide, and has become a major public health problem in contemporary society [1]. Therefore, the early and accurate diagnosis and timely treatment of breast cancer are particularly important. As a new type of breast cancer imaging technology, ultrasound CT imaging technology can invert the three-dimensional image of the internal structure of the tissue by detecting the scattered waves and reflected waves of the human tissue in the broadband frequency range, which has a high degree of biosecurity [2,3]. Therefore, the research of ultrasound CT imaging technology is of great significance for the early detection and long-term diagnosis and treatment of breast cancer [4–6].

As the core component of the ultrasound CT imaging system, the transmission and reception of ultrasound signals can be realized based on the capacitive micromachined ultrasound transducer (CMUT) [7–9]. However, due to the complexity of breast tissue, efficient acquisition of breast ultrasound signals by CMUT has become an important factor limiting accurate detection. The specific manifestations are as follows [10–14]: (1) the ultrasound signal intensity of minimal breast lesions is weak, and the acquisition is difficult; (2) the ultrasound signal transmission process is easily interfered with by the surrounding environment, and the transmission efficiency is low; (3) the limited bandwidth of the CMUT will lead to the sound waves of different frequency components to be lost during the transmission process, causing signal integrity problems; (4) the phase modulation

function is not provided by the transmission of traditional acoustic signals. Specifically, the directivity is poor, and the stable signal cannot be output. Many scholars have made efforts aiming to solve the above problems. In 2017, Zhang et al. [15] proposed the physical mechanism of dolphin beam formation, which provided a new idea for sparse CMUT arrays to achieve excellent acoustic emission directivity. In 2020, Coutant Z A et al. [16] used three sizes of square micro-elements to form CMUT array elements, achieving an increase in bandwidth. In 2021, Hani H. Tawfik et al. [17] proposed a meniscus mode, which is a new operation mechanism for signal amplification in CMUT transducers. The formation of the meniscus increases the measured signal intensity. However, as the intensity increases, the probability of meniscus rupture increases. The efficient acquisition of breast ultrasound signals is seriously affected.

The efficient transmission of breast ultrasound signals has been pointed out by the development of artificial acoustic metamaterials [18–21]. Different from the regulation mechanism of traditional artificially variable refractive index materials, the essence is to use the structure of sub-wavelength size to realize the arbitrary regulation of sound waves through fine microstructure design. Functionally, the use of metamaterials for acoustic wave modulation not only enhances the existing CMUT acquisition method, realizes multi-channel acoustic signal directional transmission, and reduces signal attenuation; it also realizes broadband transmission, phase adjustment, and other functions, laying the foundation for fast and reliable multiparameter data acquisition.

Therefore, based on acoustic metamaterials, the design of a multi-channel structure suitable for the efficient transmission of breast ultrasound signals has become a new CMUT efficient acquisition solution. Using the coupling and resonance mechanism between the sound wave and the medium in the model, the parallel directional transmission of multiple signals is realized. Therefore, the mutual interference between the signals is reduced and the transmission efficiency is effectively improved. At the same time, the acoustic signals are effectively transmitted in a wide frequency range, and more signals can be received by the CMUT. Moreover, the phase of the ultrasound signals is controlled, and the collection efficiency of CMUT is improved, which provides a data source for ultrasound tomography, and promotes research in the early screening of breast cancer.

2. Theoretical Analysis

During the acquisition of breast ultrasound signals, acoustic impedance is generated during the transmission of ultrasound in the soft tissues of the organism. Among them, the formula that best reflects the acoustic characteristics of the medium is the acoustic impedance ratio formula [22]:

$$z = \frac{\omega\rho_0}{k} = \rho_0c \quad (1)$$

In Equation (1), ω is the angular frequency, k is the wavenumber, ρ_0 is the density of the medium, and c is the speed of sound in the medium in N·s/m³.

Acoustic impedance ratio can be understood as the speed-limiting ability of the medium at a specific position in the sound field. Generally, the ultrasonic attenuation determined by the characteristics of the propagation medium obeys the law of exponential attenuation. Specifically, the relationship between the amplitude A along the propagation direction of the sound wave and the propagation distance x is:

$$A = A_0e^{-\alpha x} \quad (2)$$

In this formula, A_0 is the initial amplitude and α is the attenuation coefficient.

It can be seen that the amplitude A of the sound wave propagation direction is negatively related to the propagation distance. The greater the propagation distance, the smaller the amplitude A . Therefore, the ultrasonic signal energy is subject to attenuation during the process of transmitting information to the CMUT receiving end; the bandwidth is limited, and the complete signal cannot be collected. Acoustic metamaterials, as a kind of artificially designed composite structural materials, have the characteristics of high-

efficiency transmission of sound waves in specific frequency bands, which have a relatively large relationship with their structural characteristics. Compared with traditional acoustic materials, the cell structure of acoustic metamaterials has multiple vibration characteristics. Therefore, a specific acoustic wave transmission bandgap [23] is formed.

In 2000, Liu et al. [24] first proposed the bandgap of phononic crystals based on the local resonance mechanism. A three-dimensional, locally resonant phononic crystal was prepared by periodically inserting a lead core covered by a soft material in an epoxy resin-based material. Both theoretical and experimental results show that the limitations of the Bragg condition can be broken through, which has become an essential breakthrough in the field of phononic crystals. The local resonance type-phononic crystal bandgap is produced by the local coupling of elastic waves and oscillators.

The dispersion equation of the spring-vibrator model is [25]:

$$\omega^2 = 4KM_{eff}^{-1} \sin^2 ka \quad (3)$$

$$M_{eff} = M_1 + M_2\omega_0^2 / (\omega_0^2 - \omega^2) \quad (4)$$

$$\omega_0 = \sqrt{2G/M_2} \quad (5)$$

where M_1 and M_2 are the masses of the outer and inner layers of the double-spring vibrator, respectively. M_{eff} , ω and a represent the effective mass, the resonance frequency, and the distance between the two vibrating spheres, respectively.

In breast detection, when ultrasonic signals are transmitted through multiple channels, according to the dispersion equation of the spring-vibrator model, epoxy resin and rubber are selected as the outer layer of the metamaterial local resonance unit to achieve adjustment of the elastic coefficient. In this two-component resonance-type phononic crystal, the rubber as a scatterer assumes the role of spring and mass simultaneously [26]. Under the squeezing action of the sound wave, the epoxy resin of the matrix starts to vibrate. Under the action of elastic force, the rubber layer vibrates, which leads to the vibration of the entire structure.

In a two-dimensional phononic crystal, the propagation direction of elastic waves and sound waves is determined by the direction of the group velocity. The equation of the group velocity is as follows [27]:

$$C_{gx} = \frac{\partial \omega}{\partial k_x}, C_{gy} = \frac{\partial \omega}{\partial k_y} \quad (6)$$

In the formula, the group velocity components along the x -axis and y -axis directions are expressed: C_{gx} and C_{gy} represent the group velocity components along the x -axis and y -axis, respectively.

Therefore, in this study, a multi-channel acoustic channel model was designed based on metamaterials. The specific idea adopted in this article is: in ultrasound CT imaging, the multi-channel acoustic transmission model based on the graphene structure is used to adjust sound waves of the ultrasound signals excited by the breast tissues, and then they are received by the CMUT to achieve high-efficiency transmission of sound wave energy between human tissues and transducers. Consequently, the collection efficiency of the CMUT is improved.

3. Model Structure Design

First, the cell structure based on the acoustic metamaterial was designed. As shown in Figure 1, the rubber was placed in the epoxy resin matrix, and the width R of the rubber layer was 0.05 mm. The parameters were set as follows: $\rho_{water} = 1000 \text{ kg/m}^3$, $C_{water} = 1500 \text{ m/s}$, $\rho_{epoxyresin} = 1180 \text{ kg/m}^3$, $C_{epoxyresin} = 2540 \text{ m/s}$, $\rho_{rubber} = 1300 \text{ kg/m}^3$, $C_{rubber} = 300 \text{ m/s}$.

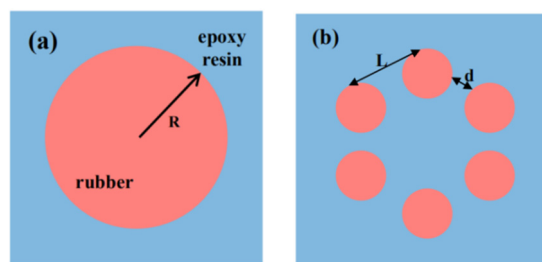


Figure 1. (a) Primitive structure; (b) graphene structure.

Graphene is a new type of two-dimensional material composed of carbon atoms, where the carbon atoms are arranged in a honeycomb regular hexagon pattern through covalent bonds. It is the thinnest two-dimensional material created so far and has good sound absorption properties [28]. To realize the regulation of the graphene structure on the sound wave, the protocell structure was arranged into the graphene structure, as shown in Figure 1b. The distance d between primitive cells is 0.1385 mm, and the length L of the sides of the hexagon is 0.2385 mm. One side is shared by the adjacent hexagons. In this paper, three columns and 16 rows of graphene structures are arranged closely to form an acoustic channel, and the thickness of the acoustic channel is 1.2 mm. As shown in Figure 2a, to study the transmission characteristics of multi-channel breast ultrasound signals, five channels were used for research in this paper.

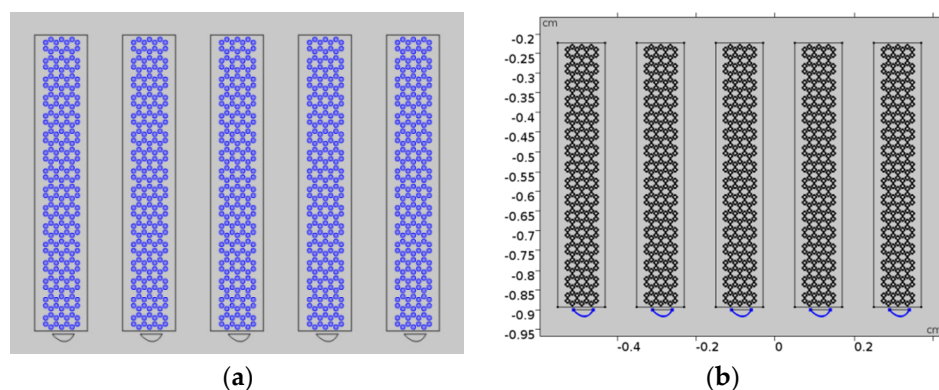


Figure 2. (a) Multi-channel breast ultrasound signal transmission model based on metamaterials; (b) parallel excitation source.

COMSOL Multiphysics, as a powerful finite element analysis software, was used to simulate the sound field signal. Based on the previous basic model [26,29–31], COMSOL finite element simulation software was used to study the transmission characteristics of breast ultrasound signals. First, the pressure acoustic transient was set, the multi-channel model was immersed in the water environment, and the hard sound field boundary was set outside. The breast ultrasound signal was simulated as a parallel excitation source, placed directly below each channel, and the sound pressure value was 2 Pa, as shown in Figure 2b. Research control-transient equations were used to solve acoustic wave equations inside the COMSOL:

$$\frac{\omega^2 p}{\rho c^2} + \nabla \cdot \left(-\frac{1}{\rho} (\nabla p_t - q_d) \right) = Q \tag{7}$$

In the formula, ρ is the density of the fluid medium, p_t is the sound pressure, q_d is a dipole source, ω is the angular frequency, c is the speed of sound in the medium, and Q is a unipolar source.

4. Results

4.1. Analysis of Acoustic Transmission Characteristics in the Time Domain

In the traditional acquisition process, when multiple sound source signals work together, the sound wave signals will interfere with each other, seriously affecting the transmission effect of ultrasonic signals. However, when there are sound channels, as shown in Figure 3, the sound wave signals are transmitted along their respective sound channels and separated from each other without diverging to the surroundings. As a result, the mutual interference and distortion of the signals are effectively reduced, and the collection efficiency is improved.

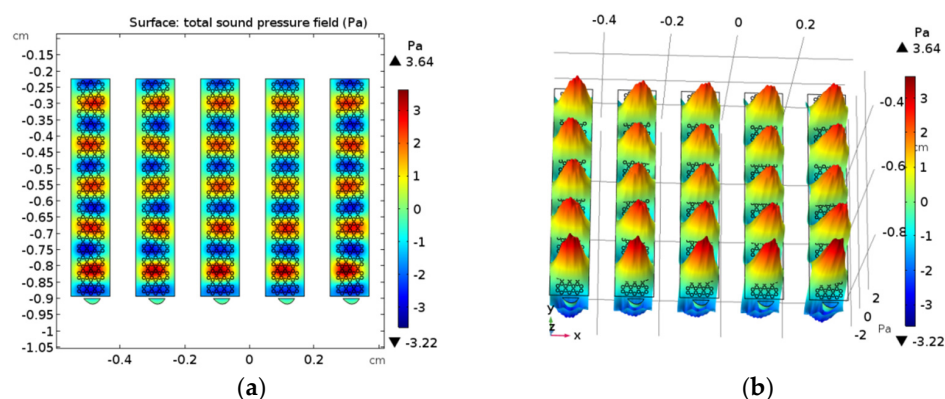


Figure 3. Transmission effect: (a) two-dimensional sound field distribution; (b) three-dimensional height expression.

To study the acoustic transmission characteristics of the acoustic channel, the time-domain transmission effect of the ultrasonic signal transmitted in the multi-channel acoustic channel was analyzed.

As shown in Figure 4, the sound pressure diagrams of the ultrasonic signals at different moments were recorded. Among them, the frequency of the sound signal was 100 kHz, and the red and blue in the sound pressure diagrams represent the sound wave signals in opposite directions. The darker the color, the greater the sound pressure value and the higher the energy. When t is $0 \mu\text{s}$, there is no sound pressure distribution inside the sound channel, and it is all green. With the increase in time, the sound wave signal is gradually transmitted along the sound channel under the action of parallel excitation. When t is $6.5 \mu\text{s}$, the sound wave is transmitted to the $1/3$ channel. Similarly, when t is $11.5 \mu\text{s}$, the sound wave is transmitted to the $2/3$ channel. The acoustic signal is transmitted from the incident port to the CMUT receiving end. Additionally, the energy is concentrated inside the model without spreading to the surroundings and gradually becomes stable after $18.25 \mu\text{s}$. In addition, during the transmission of the sound wave signal, the red and blue sound fields alternately appear, i.e., the same direction sound waves and the opposite sound waves alternately appear. This is because different metamaterial layers emit sound waves at different positions, and the phase of the sound waves emitted depends on the position of the acoustic metamaterial array. When its position is an even multiple of the half-wavelength, an in-phase acoustic wave is generated; when its position is an odd multiple of the half-wavelength, an anti-phase acoustic wave is generated. It can be seen from the sound pressure diagram that the energy value in the sound channel is much greater than the sound pressure value of the pressure source, indicating that the sound channel has a good local enhancement effect. The detection signal of minimally diseased tissue is amplified, which reduces the difficulty of detection. At the same time, the breast ultrasound signal is transmitted directionally along the acoustic channel and reaches the receiving end of the CMUT transducer without spreading to the surroundings. The collection speed of breast volume data was increased to achieve fast, real-time, high-resolution imaging.

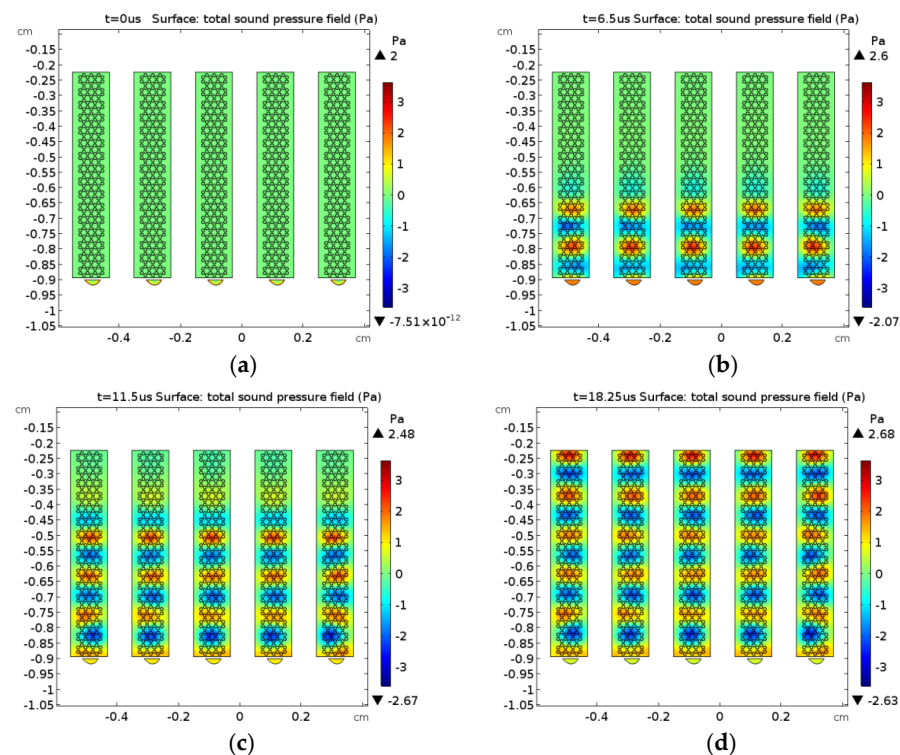


Figure 4. Simulation results in different time periods: (a) sound pressure diagram at 0 μs ; (b) sound pressure diagram at 6.5 μs ; (c) sound pressure diagram at 11.5 μs ; (d) sound pressure diagram at 18.25 μs .

To further study the change of the sound pressure value of the multi-channel sound channel model with time, under the action of the parallel excitation as shown in Figure 5a, the sound pressure change waveform of the receiving end of the five sound channels in this paper was drawn. As shown in Figure 5b, the sound pressure value at the receiving end of the CMUT was zero until 10 μs . At this time, the sound wave signal was transmitted inside the model and did not reach the receiving end. After 10 μs , as time increased, the acoustic signal gradually reached the CMUT receiving end and stabilized after 18 μs to achieve dynamic transmission. The sound wave energy was approximately 2.3 Pa, which was greater than the sound pressure value at the excitation source, achieving a good sound wave local enhancement effect and effectively amplifying the intensity of the ultrasonic signal. In the meantime, the waveforms of the five sound channels were almost the same, and they were transmitted efficiently at the same time, realizing multi-channel and efficient acquisition of sound wave signals.

4.2. The Influence of Frequency on Sound Transmission Characteristics

The frequency of the ultrasonic waves excited by the breast tissues with different degrees of variation is different, the transmission characteristics of the ultrasonic signals in different frequency bands have been further studied. As shown in Figure 6, the transmission waveforms of acoustic signals at frequencies of 80 kHz, 1000 kHz, 3000 kHz, and 4000 kHz reach the receiver of CMUT through the acoustic channel are, respectively drawn. It can be seen from the waveform that when the frequency is 80 kHz, the sound wave signal has a transmission effect in the whole process, and the sound pressure value is stable at 1.5 Pa, which has a smaller energy loss compared with the excitation source. When the sound wave frequency is 1000 kHz, the signal almost has no transmission effect before 9 μs . As time increases, the acoustic signal is gradually transmitted to the receiving end. The signal intensity is gradually enhanced and stabilized at 20 μs , and the sound pressure value is 1.4 Pa. The model cannot completely overcome the problem of sound energy loss in sound wave propagation, but it does have a stable sound wave propagation effect. When the

sound wave frequency is 3000 kHz, the sound wave transmission characteristics are similar to 1000 kHz. With the increase in frequency, the amplitude of attenuation is increased gradually, and the oscillation effect is stronger. When the sound wave frequency is 4000 kHz, the sound wave intensity is small, oscillating around 0.05 Pa. The transmission effect is weak and can be ignored. Therefore, the acoustic signal can be effectively transmitted in the 80 kHz to 4000 kHz band, and broadband transmission is realized. More acoustic signals with different frequency components are delivered to the receiving end, and the signal integrity is improved. It can be seen that through the multi-channel acoustic channel model designed in this article, the effective transmission bandwidth is increased, and the integrity of the collected signal is improved.

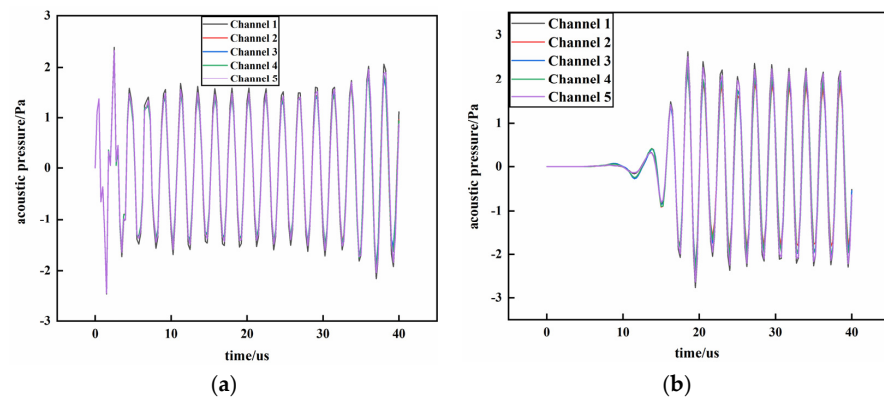


Figure 5. (a) Five-channel incident sound pressure change; (b) five-channel exit sound pressure change.

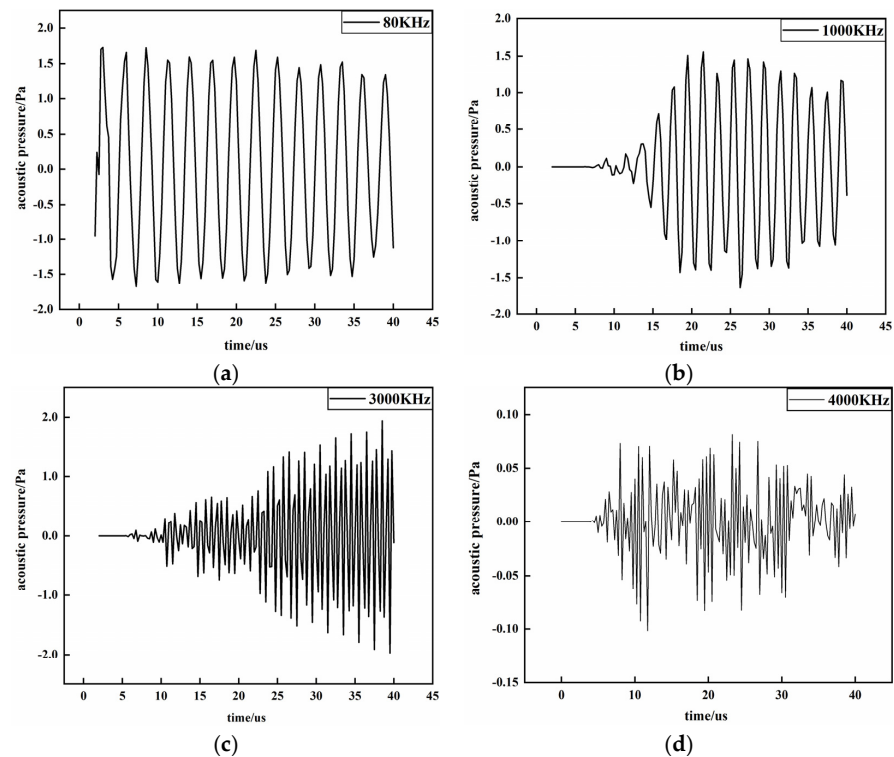


Figure 6. Transmission waveforms at different frequencies: (a) Sound pressure graph at 80 kHz; (b) Sound pressure graph at 1000 kHz; (c) Sound pressure graph at 3000 kHz; (d) Sound pressure graph at 4000 kHz.

4.3. The Influence of Structural Parameters on Sound Wave Transmission Characteristics

With better directional properties in the CMUT cylinder array, a more stable ultrasonic signal would be produced, the reception performance of CMUT would be improved, and the receiving efficiency of the CMUT would be improved. By studying the influence of structural parameters on signal transmission characteristics, phase modulation was achieved.

With other parameters unchanged, the frequency of the five input ultrasonic signals was 100 kHz, the amplitude was 2 Pa, and the phase difference as $3\pi/8$. The period of the incident sound pressure function of one channel was $3\pi/2$, and the phases of other channels were shifted to the right by $3\pi/8$, $3\pi/4$, $9\pi/8$, $3\pi/2$ and in turn.

Figure 7a shows the simulation of the ultrasonic signal at different input signals. It can be seen from the simulation diagram that the sound pressure distribution at the peak and trough of the output sound pressure is messy, and there is an obvious phase difference. On this basis, the subject changed the structural parameters of the material to achieve phase modulation. As shown in Figure 7b, the phase of the acoustic signal can be distributed regularly. The acoustic wavefront arriving at the exit point has the same phase, i.e., constructive interference occurs. Therefore, despite the different directions and paths, after different ultrasonic signals are processed through the acoustic channel, the phase can be adjusted to deflect the beam and output a stable ultrasonic signal under the action of phase modulation. Moreover, the signal is transmitted along the channel, the pointing performance is improved, and the transmission efficiency of breast ultrasound signals is greatly enhanced, which is conducive to efficient acquisition and high-resolution ultrasound imaging.

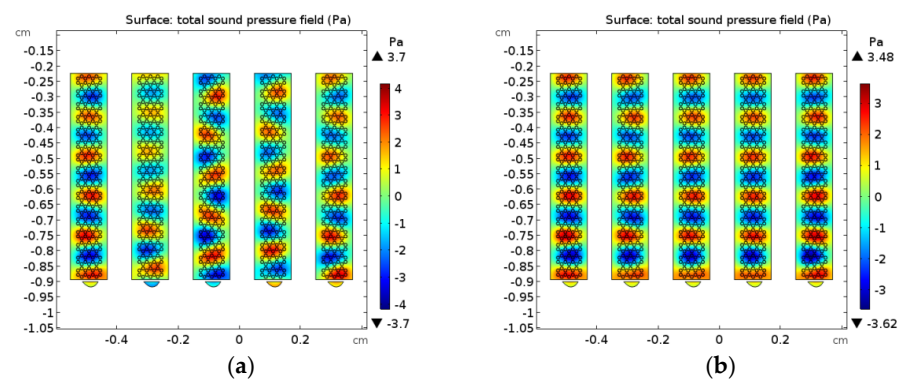


Figure 7. (a) Sound field distribution before phase modulation; (b) sound field distribution after phase modulation.

In short, based on the bandgap theory of phononic crystals, the efficient transmission of ultrasound signals was realized by the multi-channel breast ultrasound signal model designed in the simulation. In 2008, Yang et al. [31] experimentally proposed and prepared a two-dimensional membrane–mass structure negative-mass-density acoustic metamaterial, and systematically studied the singular properties of the acoustic metamaterial based on this structure. The feasibility of the multi-channel model design was confirmed by this experiment, which provided a new idea for the efficient transmission of breast ultrasound signals.

5. Conclusions

In ultrasound CT imaging, there are problems such as low ultrasound signal transmission efficiency and severe interference. In this article, based on the graphene structure and acoustic metamaterials, a multi-channel acoustic channel model designed by COMSOL was proposed to achieve the efficient transmission of breast ultrasound signals, thereby achieving the efficient acquisition of CMUT. Through the analysis of the efficient transmission characteristics of sound waves, the following conclusions can be drawn.

- (1) When the frequency of the acoustic signal is 100 kHz, the acoustic signals are transmitted along their respective acoustic channels and separated from each other without diverging, which effectively reduces the mutual interference and distortion of the signals. Simultaneously, the energy of the ultrasonic signal reaching the receiving end of the CMUT through the acoustic channel is enhanced, which reduces the difficulty of acquisition and provides the possibility for accurate detection of early breast cancer.
- (2) For sound wave signals of different frequencies, they can be effectively transmitted when passing through the sound channel in the wide frequency range of 80 kHz to 4000 kHz. The transmission frequency band of the acoustic signal is effectively expanded, and the integrity of the signal arriving at the receiving end of the CMUT is improved, realizing efficient acquisition.
- (3) Based on the flexibility of the phononic crystal structure design, changing the parameters of the primitive cell structure, the phase adjustment can be realized in a wide frequency range, which greatly enriches the function of the acoustic channel. The beam is deflected by adjusting the phase to improve directivity, and the efficient acquisition of CMUT is better realized, providing a database for accurate diagnoses of breast cancer.

Author Contributions: Methodology, X.Z.; software, P.Y.; validation, X.Z., R.Z. and J.H.; formal analysis, R.Z.; resources, J.H.; writing—original draft preparation, X.Z.; writing—review and editing, P.Y.; supervision, J.H.; funding acquisition, J.H. All authors have read and agreed to the published version of the manuscript.

Funding: This research was funded by The National Natural Science Foundation of China, grant number 61671414, The National Nature Science Foundation of China as National Major Scientific Instruments Development Project, grant number 61927807, and The Postdoctoral Science Foundation of China, grant number 2017M611198.

Institutional Review Board Statement: “Not applicable” for studies not involving humans or animals. This study is only the signal simulation analysis and there is no experiment part.

Informed Consent Statement: “Not applicable” for studies not involving humans.

Data Availability Statement: The data presented in this study are openly available in web of science.

Acknowledgments: The work was supported by The National Natural Science Foundation of China (61671414), The National Nature Science Foundation of China as National Major Scientific Instruments Development Project (61927807), and The Postdoctoral Science Foundation of China (2017M611198).

Conflicts of Interest: The authors declare no conflict of interest. The funders had role in the writing of the manuscript or in the decision to publish the results.

References

1. Koboldt, D.; Fulton, R.; McLellan, M.; Schmidt, H.; Kalicki-Veizer, J.; McMichael, J.; Fulton, L.; Dooling, D.; Ding, L.; Mardis, E.; et al. Comprehensive molecular portraits of human breast tumours. *Nature* **2012**, *490*, 61–70.
2. Nebeker, J.; Nelson, T.R. Imaging of sound speed using reflection ultrasound tomography. *J. Ultrasound Med.* **2012**, *31*, 1389–1404. [[CrossRef](#)] [[PubMed](#)]
3. Bernard, S.; Monteiller, V.; Komatitsch, D.; Lasaygues, P. Ultrasonic computed tomography based on full-waveform inversion for bone quantitative imaging. *Phys. Med. Biol.* **2017**, *62*, 7011–7035. [[CrossRef](#)]
4. Forte, S.; Dellas, S.; Stieltjes, B.; Bongartz, B. Multimodal ultrasound tomography for breast imaging: A prospective study of clinical feasibility. *Springer Int. Publ.* **2017**, *1*, 27. [[CrossRef](#)]
5. Liu, C.; Xue, C.; Zhang, B.; Zhang, G.; He, C. The Application of an Ultrasound Tomography Algorithm in a Novel Ring 3D Ultrasound Imaging System. *Sensors* **2018**, *18*, 1332. [[CrossRef](#)] [[PubMed](#)]
6. Yu, S.; Wu, S.; Zhuang, L.; Wei, X.; Sak, M.; Neb, D.; Hu, J.; Xie, Y. Efficient Segmentation of a Breast in B-Mode Ultrasound Tomography Using Three-Dimensional GrabCut (GC3D). *Sensors* **2017**, *17*, 1827. [[CrossRef](#)] [[PubMed](#)]
7. Ergun, A.; Yaralioglu, G.; Khuri-Yakub, B. Capacitive Micromachined Ultrasonic Transducers: Theory and Technology. *J. Aerosp. Eng.* **2003**, *16*, 76–84. [[CrossRef](#)]
8. Park, K.; Lee, H.; Kupnik, M.; Khuri-Yakub, B. Fabrication of Capacitive Micromachined Ultrasonic Transducers via Local Oxidation and Direct Wafer Bonding. *J. Microelectromech. Syst.* **2011**, *20*, 95–103. [[CrossRef](#)]

9. Yu, Y.; Vai, M.; Mak, P.; Cao, X.; Pun, S. Output pressure enhancement of CMUTs by using multiple Helmholtz resonance apertures. *Electron. Lett.* **2015**, *51*, 1390–1392. [[CrossRef](#)]
10. Zhu, Y.; Hu, J.; Fan, X.; Yang, J.; Liang, B.; Zhu, X.; Cheng, J. Fine manipulation of sound via lossy metamaterials with independent and arbitrary reflection amplitude and phase. *Nat. Commun.* **2018**, *9*, 1632. [[CrossRef](#)]
11. Terada, T.; Yamanaka, K.; Suzuki, A.; Tsubota, Y.; Wu, W.; Kawabata, K. Highly precise acoustic calibration method of ring-shaped ultrasound transducer array for plane-wave-based ultrasound tomography. *Jpn. J. Appl. Phys.* **2017**, *56*, 07JF07. [[CrossRef](#)]
12. Fei, C.; Ma, J.; Chiu, C.; Williams, J.; Fong, W.; Chen, Z.; Zhu, B.; Xiong, R.; Shi, J.; Hsiai, T.; et al. Design of matching layers for high-frequency ultrasonic transducers. *Appl. Phys. Lett.* **2015**, *107*, 123505. [[CrossRef](#)]
13. Song, J.; Xue, C.; He, C.; Zhang, R.; Mu, L.; Cui, J.; Miao, J.; Liu, Y.; Zhang, W. Capacitive Micromachined Ultrasonic Transducers (CMUTs) for Underwater Imaging Applications. *Sensors* **2015**, *15*, 23205–23217. [[CrossRef](#)] [[PubMed](#)]
14. Zhang, R.; Zhang, W.; He, C.; Song, J.; Mu, L.; Cui, J.; Zhang, Y.; Xue, C. Design of capacitive micromachined ultrasonic transducer (CMUT) linear array for underwater imaging. *Sens. Rev.* **2016**, *36*, 77–85. [[CrossRef](#)]
15. Zhang, Y.; Gao, X.; Zhang, S.; Cao, W.; Tang, L.; Wang, D.; Li, Y. A biomimetic projector with high subwavelength directivity based on dolphin biosonar. *Appl. Phys. Lett.* **2014**, *105*, 123502. [[CrossRef](#)]
16. Coutant, Z.; Adelegan, O.; Biliroglu, A.; Jeng, G.; Oralkan, O. Wideband Air-Coupled CMUT Arrays for Acoustic Micro-Tapping. In Proceedings of the 2020 IEEE International Ultrasonics Symposium (IUS), Las Vegas, NV, USA, 7–11 September 2020.
17. Tawfik, H.; Singh, N.; Elsayed, M.; Nabki, F.; El-Gamal, M.N. Meniscus-Mode: A Novel Operation Mechanism for Signal Amplification in Capacitive Micromachined Ultrasonic Transducers. *Sen. Act. A Phys.* **2021**, *319*, 112549. [[CrossRef](#)]
18. Yang, S.; Page, J.; Liu, Z.; Cowan, M.; Chan, C.; Sheng, P. Focusing of sound in a 3D phononic crystal. *Phys. Rev. Lett.* **2004**, *93*, 024301. [[CrossRef](#)]
19. Ding, Y.; Liu, Z.; Qiu, C.; Shi, J. Metamaterial with simultaneously negative bulk modulus and mass density. *Phys. Rev. Lett.* **2007**, *99*, 093904. [[CrossRef](#)] [[PubMed](#)]
20. Tang, S.; Wang, R.; Han, J.; Jiang, Y. Acoustic energy transport characteristics based on amplitude and phase modulation using waveguide array. *J. Appl. Phys.* **2020**, *128*, 165103. [[CrossRef](#)]
21. Li, K.; Liang, B.; Yang, J.; Yang, J.; Chen, J. Broadband transmission-type coding metamaterial for wavefront manipulation for airborne sound. *Appl. Phys. Express* **2018**, *11*, 077301. [[CrossRef](#)]
22. Li, Y.; Hou, Z.; Oudich, M.; Assouar, M. Analysis of surface acoustic wave propagation in a two-dimensional phononic crystal. *J. Appl. Phys.* **2012**, *112*, 023524. [[CrossRef](#)]
23. Liu, Z.; Chan, C.; Sheng, P. Three-component elastic wave band-gap material. *Phys. Rev. B* **2002**, *65*, 1651161–1651166. [[CrossRef](#)]
24. Liu, Z.; Zhang, X.; Mao, Y.; Zhu, Y.; Yang, Z.; Chan, C.; Sheng, P. Locally resonant sonic materials. *Science* **2000**, *289*, 1734–1736. [[CrossRef](#)] [[PubMed](#)]
25. Tang, S.; Han, J.; Wen, T. Directional acoustic transmission based on metamaterials. *AIP Adv.* **2018**, *8*, 085312. [[CrossRef](#)]
26. Wang, G.; Wen, X.; Wen, J.; Shao, L.; Liu, Y. Two-Dimensional Locally Resonant Phononic Crystals with Binary Structures. *Phys. Rev. Lett.* **2004**, *93*, 154302. [[CrossRef](#)]
27. Wen, J.; Cai, L.; Yu, D.; Xiao, Y.; Zhao, H.; Yin, J.; Yang, H. *Basic Theory and Application of Acoustic Metamaterials*; Science Press: Beijing, China, 2018; pp. 91–92.
28. Yang, P.; Wu, J.; Zhao, R.; Han, J. Study of high frequency acoustic directional transmission model based on graphene structure. *AIP Adv.* **2020**, *10*, 035308. [[CrossRef](#)]
29. Zhao, X.; Yang, P.; Zhao, R.; Han, J. Research on acoustic conduction mechanism of underwater acoustic channel based on metamaterials. *AIP Adv.* **2020**, *10*, 115321. [[CrossRef](#)]
30. Yang, P.; Wu, J.; Zhao, R.; Han, J. Research on Local Sound Field Control Technology Based on Acoustic Metamaterial Triode Structure. *Crystals* **2020**, *10*, 204. [[CrossRef](#)]
31. Yang, Z.; Mei, J.; Yang, M.; Chan, N.; Sheng, P. Membrane-Type Acoustic Metamaterial with Negative Dynamic Mass. *Phys. Rev. Lett.* **2008**, *101*, 204301. [[CrossRef](#)]